The 2023/24 El Niño and the Feasibility of Long-Lead ENSO Forecasting

Desislava Petrova,[a] Xavier Rodó,[a,b] Siem Jan Koopman,[c] Vassil Tzanov,[d] Ivana Cvijanovic, [a]

[a] Barcelona Institute for Global Health (ISGlobal), Climate and Health Program, Barcelona, Catalonia, Spain

[b] ICREA, *Barcelona, Catalonia, Spain*

[c] Vrije Universiteit, *Department of Econometrics, Amsterdam, the Netherlands*

[d] Universitat Rovira i Virgili, *the Public University of Tarragona, Department of Inorganic Chemistry, Tarragona, Catalonia, Spain*

Corresponding author: Desislava Petrova, desislava.petrova@isglobal.org

ABSTRACT

Through its atmospheric teleconnections, El Niño Southern Oscillation (ENSO) shifts and disrupts weather and climate patterns far beyond the equatorial Pacific where it occurs, and occasionally has catastrophic consequences in many countries of the world. It is also the largest source of seasonal and interannual climate predictability. Despite its huge importance, ENSO forecasting is still not performed operationally at longer leads than about 6 months ahead. At the same time, there is mounting scientific evidence that forecasts are possible even more than a year in advance. Early warning of ENSO could substantially mitigate and help avoid some of the most damaging impacts, such as floods, droughts, harvest failure, famine, migration and disease outbreaks. Here, we present forecasts from a statistical ENSO model of the next El Niño predicted to occur in the winter of 2023/24, at lead times between 11 and 17 months ahead of an expected peak in December 2023. We use a statistical unobserved dynamic components model (EDCM) based on subsurface ocean temperatures as well as sea surface temperatures and zonal wind stress. EDCM has been previously validated through hindcasts of the major El Niños since 1970, and through real time forecasts of the 2015/16 and 2018/19 El Niños. Our statistical method and results indicate that there is potential for doubling the operational predictive lead time of ENSO to at least 12 months, with additional promise for even earlier anticipation of 19 months. Such longer-lead forecasts could be of high value, because decision-making and management in a number of key socio-economic sectors could be greatly improved.

SIGNIFICANCE STATEMENT

We employ a statistical ENSO model and show early forecasting of the 2023 El Niño (EN). Early forecasts initiated in May and July 2022 predicted a mild EN. Forecasts initiated later, in November 2022 and January 2023, predicted a moderate EN, with a strong event falling within the 70% confidence intervals. This work confirms that statistical long-lead ENSO forecasts are feasible, and should be developed further in advance of the operational threshold of 6-8 months. Such forecasts are of high value for agriculture, water management, disaster reduction, public health and energy production in countries affected by ENSO. More so, a strong EN could lead to a temporary breach of the 1.5°C threshold for global mean temperature increase set in the Paris Climate Agreement.

CAPSULE (BAMS ONLY)

We predicted that El Niño will occur in the winter of 2023/24 at longer lead times (11-17 months in advance) compared to the operational forecasts of 6-8 months ahead.

1. Introduction

El Niño Southern Oscillation (ENSO) and its predictability is a subject of widespread scientific and societal interest, both because of its complexity as the dominant atmosphere-ocean coupled mode of climate variability (Wyrtki, 1975, Philander 1983), and its links to multiple climate hazards worldwide (Sarachik and Cane, 2010). A large number of ENSO prediction models have been described in the literature, and the operational ENSO forecasting plume includes contributions from many statistical and dynamical models (Barnston et al. 2012). Official forecasts are issued and reported regularly by the International Research Institute for Climate and Society Earth Institute (IRI, https://iri.columbia.edu/our-expertise/climate/enso/), and by the National Atmospheric and Oceanic Administration and the Climate Prediction Center (NOAA/CPC,https://www.cpc.ncep.noaa.gov/products/analysis_monitoring/enso_advisory/) about two seasons in advance. However, ENSO forecasting is currently not performed operationally at longer lead times (beyond 6 months in advance), despite the growing number of studies indicating that a longer predictability range is feasible (Cane et al. 1986; Goswami and Shukla 1991; Latif et al. 1998; Chen and Cane 2008; Wittenberg et al. 2014; Gonzalez and Goddard 2016; Luo et al. 2016; DiNezio et al. 2017; Astudillo et al. 2017). Given that the ENSO forecasts are also the largest source of seasonal precipitation and temperature predictability for the Pacific and North Atlantic regions, North and South America, Australia, the Maritime Continent, and parts of Asia and Africa (Ropelewski and Halpert 1987, Rodó et al. 2006, Sarachik and Cane 2010, Kumar et al. 2017, L'Heureux et al. 2020), early anticipation through long-lead forecasts could have huge economic, societal and health benefits that are currently underutilized.

A handful of studies have already documented long-lead forecasts of past ENSO events (Latif et al. 1998; Chen et al. 2004; Luo et al. 2008; Izumo et al. 2010; Ludescher et al. 2013, 2014; Petrova et al. 2017; Gonzalez and Goddard 2016; Ramesh et al. 2017; Luo et al. 2017; Meng et al. 2020, Petrova et al. 2020), with the majority of these being based on dynamical models. In the 1980s and 1990s substantial efforts were made to implement a monitoring system within the Tropical Ocean Global Atmosphere (TOGA) Program, formed by a three-dimensional array that regularly samples the surface and subsurface temperature, salinity and circulation in the tropical Pacific, with the specific aim to understand the physical mechanisms of ENSO better, and to improve its prediction (McPhaden and Yu 1999). As a result, forecasts from dynamical models have significantly improved since 1985. However, the majority of the operational statistical models do not utilize the more detailed subsurface information provided by the observation system, which could effectively help improve predictions further (Barnston et al. 2012). A novel dynamic components statistical ENSO model (EDCM) was developed and described by Petrova et al. 2017 and 2020 which, along with surface zonal wind stress and temperature, specifically samples subsurface temperature information from the western and central equatorial Pacific Ocean (WPAC and CPAC) to predict ENSO events at lead times beyond one year in advance. The EDCM has successfully hindcasted all major El Niños (EN) since 1970 at leads of up to about 2 years in advance (Petrova et al. 2020), demonstrating that such predictive lead times are possible also for statistical models. Moreover, the last few EN, i.e. the 2014-2016, and the 2018-2020 events were predicted in operational forecasting mode (see Petrova et al. 2017, Lowe et al. 2017, Petrova et al. 2020, Petrova et al. 2021). These long-lead EN forecasts were used within a dengue fever incidence model for the city of Machala in Ecuador, to assess the probability of a dengue outbreak up to 11 months in advance (Lowe et al. 2017, Petrova et al. 2021). In this way, EDCM was not only tested in real-time, but its potential to extend the forecast lead time of a climate-sensitive disease was also demonstrated.

When the first ENSO forecasts became a reality in the second half of the 1980s, it also became obvious that such predictions could facilitate the generation of seasonal climate forecasts, as well as their application for practical uses (Buizer et al. 2009). ENSO associated droughts and flooding worldwide could be predicted some months in advance, and the hope was that these predictions could help, for example, vulnerable farming communities to prepare and plant more resilient crops, and governments to save precious resources when planning for response to natural hazards. Nowadays, many institutions around the globe (including IRI) tailor and provide climate information and decision support systems on seasonal and interannual time scales to the agricultural, health, energy, insurance, disaster reduction and other sectors of society impacted by climate variability and change. However, despite the immense practical utility of ENSO forecasts, attempts to issue predictions at longer lead times, beyond the traditional 6 months in advance, have only been restricted to the scientific undertaking, and none are issued on an operational level yet.

In the present study we use EDCM to perform in real-time statistical predictions of the temperatures in the eastern equatorial Pacific for the winter of 2023/24 at increasing lead times of up to 19 months in advance, and we investigate the potential of such longer lead forecasts in assisting the climate impact community, decision-makers around the world, and ultimately society, in alleviating the negative impacts of ENSO. We describe the predictors and the dynamic components of the model in Section 2. We summarize the ENSO forecasts in Section 3, and discuss the results and implications of these longer leads for climate impacts and services in Section 4.

2. Methods

Here we apply EDCM, the statistical ENSO time series prediction model, based on dynamic unobserved components derived from the decomposition of the Niño3.4 temperature time series, and described in detail in Petrova et al. 2017 and 2020, to predict the monthly temperature in the Niño3.4 region ([5°N - 5°S]*x*[170° - 120°W]) for the 2023/24 boreal winter season. The model includes a trend component, a seasonal component, and three cyclical components with different frequencies and variances, as well as a number of regression (predictor) variables, and a noise term. Given that the model includes a trend component, a detrending of the Niño3.4 temperature and predictor time series is not necessary. The trend, seasonal, and cycle components are represented as linear dynamic stochastic processes driven by disturbances (Harvey and Koopman 2000, Durbin and Koopman 2012). The cycle components are estimated with periods corresponding to near-annual (NA), quasi-biannual (QB) and quasi-quadrennial (QQ) frequencies, which are typical modes of ENSO variability discussed at length in the literature (see Petrova et al. 2017 and 2020 and the references therein). The signal extraction of the different components, the likelihood evaluation, and the actual ENSO forecasting are achieved by means of the Kalman Filter (Kalman 1960). The statistical estimations and forecast method are implemented and carried out by the software packages STAMP and OxMetrics (Koopman et al. 2008 and 2010, Doornik 2013).

Predictions are initiated at particular lead times with respect to December 2023 (as it is generally assumed that ENSO events peak around December). We look at predictive lead times beyond boreal spring, in order to test the skill of the model to overcome the well-known ENSO spring “predictability barrier” (Torrence and Webster 1998, Sarachik and Cane 2010). Therefore, forecasts are initiated between 11 and 19 months ahead of a presumed December 2023 ENSO peak, i.e. between the months of May 2022 and January 2023. As discussed in detail in Petrova et al. 2017, EDCM makes use of different predictors at different lead times, ranging from subsurface temperature at different depth levels, sea surface temperatures (SST), as well as zonal wind stress (Supplementary Tables S1 and S2). These predictor indices (their time series) are based on the general progression of a typical El Niño event (EN), and are extracted from predefined regions in the western and central equatorial Pacific (WPAC and CPAC; Petrova et al. 2017). Intensification of the trade winds and a subsurface heat buildup in the WPAC, and its slow subsurface migration towards the CPAC, along with westerly wind bursts at a later stage, are well-known to play a key role in the onset of El Niño events (Wyrtki 1985; Cane et al. 1986; Jin 1997; Clarke and Van Gorder 2003; McPhaden 2003, 2004; McPhaden et al. 2006; Ramesh and Murtugudde 2013; Ballester et al. 2015 and 2016a; Petrova et al. 2017). In this regard, EDCM benefits from available subsurface data to represent in detail these dynamical processes and their interactions. In addition to these predictor variables, we also use a previously identified SST dipole pattern in the extratropical South Pacific called the RossBell dipole (RB SST) as an ENSO predictor at a lead time of 11 months (i.e. for the forecast started in January 2023). The dipole was first defined in Ballester et al. 2011, and it represents a difference in SST warm and cold anomalies preceding EN events near the Ross and Bellingshousen Seas, respectively (over the boxes [65° - 50°S]*x*[180° - 160°W] and [65° - 50°S]*x*[100° - 80°W]). Its potential as an ENSO predictor at a lead time of between 7-11 months has been discussed therein and in Petrova et al. 2024. In particular RB peaks are followed by EN events approximately 9 months later. On the other hand, RB is anticipated by warming in the western equatorial Pacific about an year in advance. Namely, the western equatorial surface warming triggers an intensification of the local convection and upper tropospheric divergence, generating an eastward and poleward propagating atmospheric wavetrain in the southern extratropics (Ballester et al. 2011, Cvijanovic et al. 2017). This wavetrain triggers the local SST anomalies that form the RB dipole in the south Pacific. RB has also been used to predict other EN events within EDCM such as the 2009/10 and the 2015/16 EN (not shown).

For SST data we used the *NOAA OISST V2* (Reynolds et al. 2002; http://www.emc.ncep.noaa.gov/research/cmb/sst_analysis/); for subsurface temperature data the Hadley Centre EN4.2.2 analyses data with the .g10 bias correction (Good et al. 2013, Gouretski and Reseghetti 2010, Gouretski and Cheng 2020); and for the calculation of zonal wind stress we used the NCEP-NCAR reanalysis wind data (Kalnay et al. 1996).

3. Results

a. Climate conditions in the tropical Pacific in 2022 and the beginning of 2023

Figure 1a shows the average SST anomalies for the months between July and October 2022. Visible are the cold La Niña-related anomalies in the EPAC and CPAC, as well as a prominent warm anomaly in the North Pacific. Of interest here is the less intense, but significant warm anomaly (Supplementary Fig. 1a shows the standardized SST anomalies) in the far WPAC, extending south of the equator (selected by the red box). It has been shown previously that warm SST anomalies in this area typically precede El Niño events on average about 14-18 months in advance (Ballester et al. 2011 and 2016a, Petrova et al. 2017). The region highlighted in the red box in Figure 1a is the region from which we extract SSTs to use as a predictor in EDCM. We highlight that the grid-point maximum warm anomaly inside the box reaches ~2°C, and is located just to the south of the equator. The time series of this predictor index is shown in Figure 1c. Since the index represents an average temperature value over the whole box, it indicates a lower value than 2°C. The blue arrows highlight the warm anomaly peaks that preceded past EN events, and a peak is also highlighted in July-October of 2022.

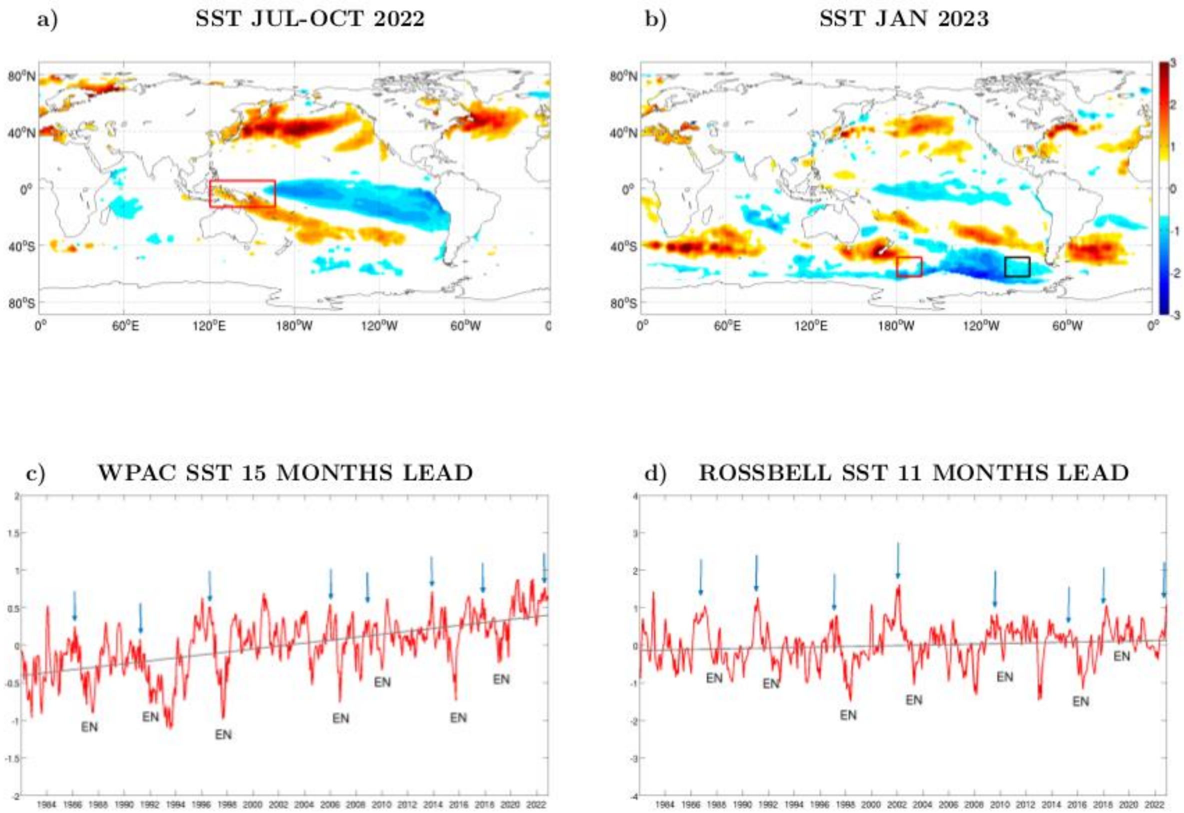

Fig. 1: Surface oceanic conditions in 2022 and the beginning of 2023 conducive to El Niño, and SST time series of the predictors used in the EDCM model at lead times of 15 and 11 months. a) and b) Sea surface temperature (SST) anomalies [ºC], c) SST anomalies

extracted from the box [10ºS-0º]x[140º-160ºE], d) RossBell SST index. Red and black boxes in panels a-b include regions from which SST predictors have been extracted for EDCM at different lead times with respect to the winter 2023/24 peak season. Arrows in panels c-d indicate the time when a predictor is used for forecasting. “EN” labels indicate the time of peak El Niño conditions. Linear trend lines are included for the time series in panels c) and d) as grey solid lines. The period used to calculate a climatology is 1982-2022.

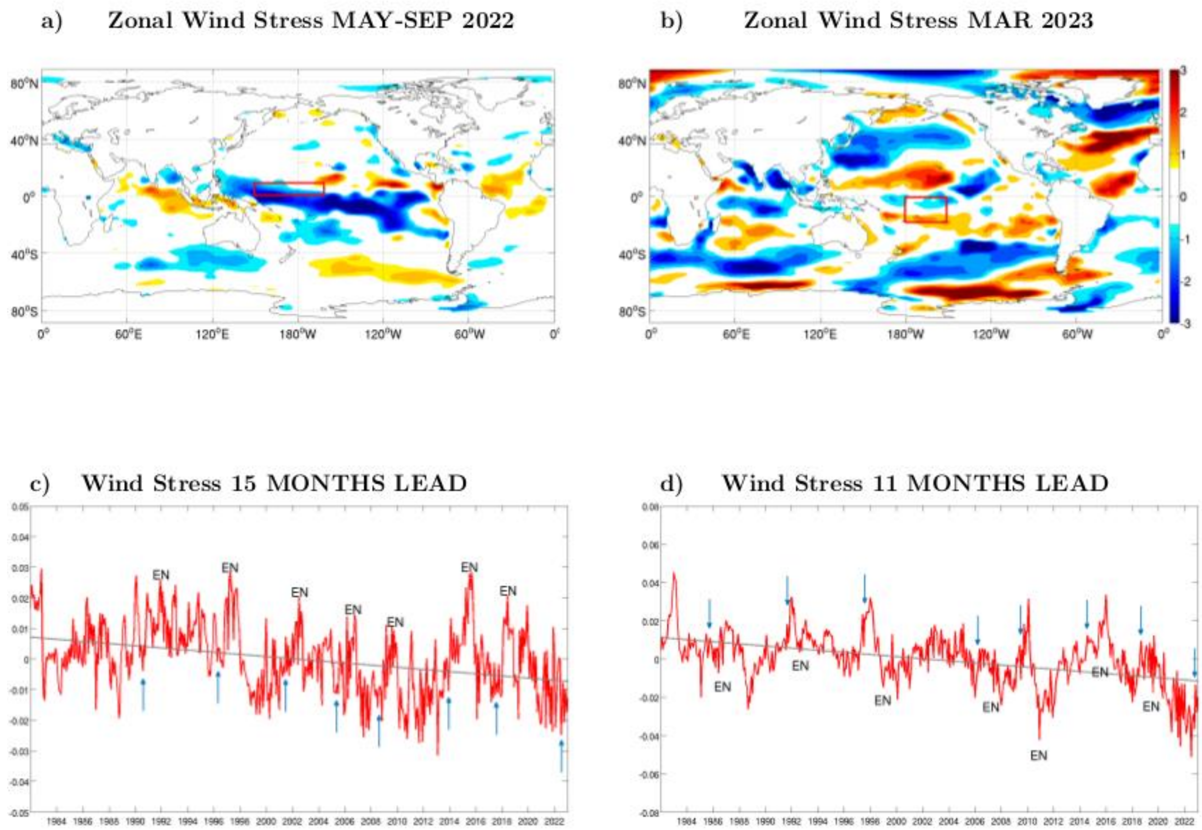
a) Zonal Wind Stress MAY-SEP 2022
b) Zonal Wind Stress MAR 2023
80°N
40°N
0°
40°S
80°S
0°
60°E
120°E
180°W
120°W
60°W
c) Wind Stress 15 MONTHS LEAD
d) Wind Stress 11 MONTHS LEAD
EN

Fig. 2: Surface atmospheric conditions in 2022 and the beginning of 2023 conducive to El Niño, and zonal wind stress time series of the predictors used in the EDCM model at lead times of 15 and 11 months. a) and b) Standardized zonal wind stress anomalies [standard deviation], c) zonal wind stress [N/m^2] extracted from the box [0º-10ºN]x[160º-200ºE], d) zonal wind stress [N/m^2] extracted from the box [10ºS-0º]x[180º-210ºE]. Red boxes in panels a-b include regions from which zonal wind stress predictors have been extracted for EDCM at different lead times with respect to the winter 2023/24 peak season. Arrows in panels c-d indicate the time when a predictor is used for forecasting. "EN" labels indicate the time of peak El Niño conditions. Linear trend lines are included for the time series in panels c) and d) as grey solid lines. The period used to calculate a climatology is 1982-2022.

Similarly, Figure 1b shows the SST anomalies in January 2023, and the RB dipole feature in the South Pacific is captured by the red and black boxes. The boxes do not encompass the areas of the strongest warm and cold anomalies, but we note that these anomalies generally progress eastwards with the evolution of EN, and peak in the two boxed regions about 7-9 months before the ENSO peak (i.e. in the months of March-May; Ballester et al. 2011). At the time of writing, the data is only available until January 2023, but it can be inferred from Figure 1b (Supplementary Fig. 1b) that the anomalies may be better captured by our boxes in the months of March-May 2023, as a result of the general eastward propagation of these features (Ballester et al. 2011). The RB dipole time series is shown in Figure 1c and a prominent peak is also highlighted at the very end of the time series in January 2022.

Standardized zonal wind stress anomalies in 2022 and the beginning of 2023 are depicted in Figure 2, panels a and b. Panel a shows that strong easterly wind anomalies occurred in the period between May and September of 2022, peaking in the far WPAC region, as well as south of the equator towards the CPAC and EPAC. Strong easterly wind anomalies at these locations precede EN events on average by about 15-20 months in advance. Although our red box does not include the entire area of strong trade wind anomalies, it does capture a significant portion of it. The zonal wind stress time series extracted from the box-marked region is shown in Figure 2c. A large trough indicative of easterly wind bursts is highlighted in the autumn months of 2022, also signaling the potential for a forthcoming EN event. We note that the biggest troughs in Figure 2c are not always associated with EN events. The EDCM predictive framework includes other statistical criteria to pinpoint the lead time at which a given predictor is the most significant. In January of 2023 (Figure 2b) the extended warm SST anomalies in the WPAC region generated some westerly wind anomalies in the south, but also in the north off-equatorial regions in the CPAC, features that are typical about 7-11 months prior to EN events (Eisenman et al. 2005). The red box in Figure 2b captures some of these westerly wind burst anomalies. The time series of the predictor extracted from this box is shown in Figure 2d, and a peak associated with westerly wind bursts at the end of the time series in December-January 2022/23 is highlighted.

Figure 3 depicts the subsurface temperature anomalies at different depths and in different months between May and October 2022, along with boxes from which predictors for EDCM were extracted. Strong warm anomalies in the WPAC are observed between 150-300 meters depth in May, July and September of 2022, which gradually progress eastward and are already stronger in the CPAC subsurface in October 2022 (Figure 3g). The subsurface temperature time series predictors extracted from the black boxes in Figure 3a and g are shown in Figure 3b and d, and the predictors used at 12 and 13 months leads are also shown in Figure 3f and h. As seen in all panels b, d, f and h of Figure 3, prominent and sustained positive peaks occur in all the time series of subsurface temperature anomalies from the spring to the winter months of 2022. Such strong subsurface warm anomalies always precede EN events by on average 10-20 months (McPhaden 2004, Ramesh and Murtugudde 2013, Petrova et al. 2017). Thus, climate conditions broadly spanning the spring, summer, autumn and winter months of 2022/23 are collectively prime for a forthcoming EN event in the winter of 2023/24.

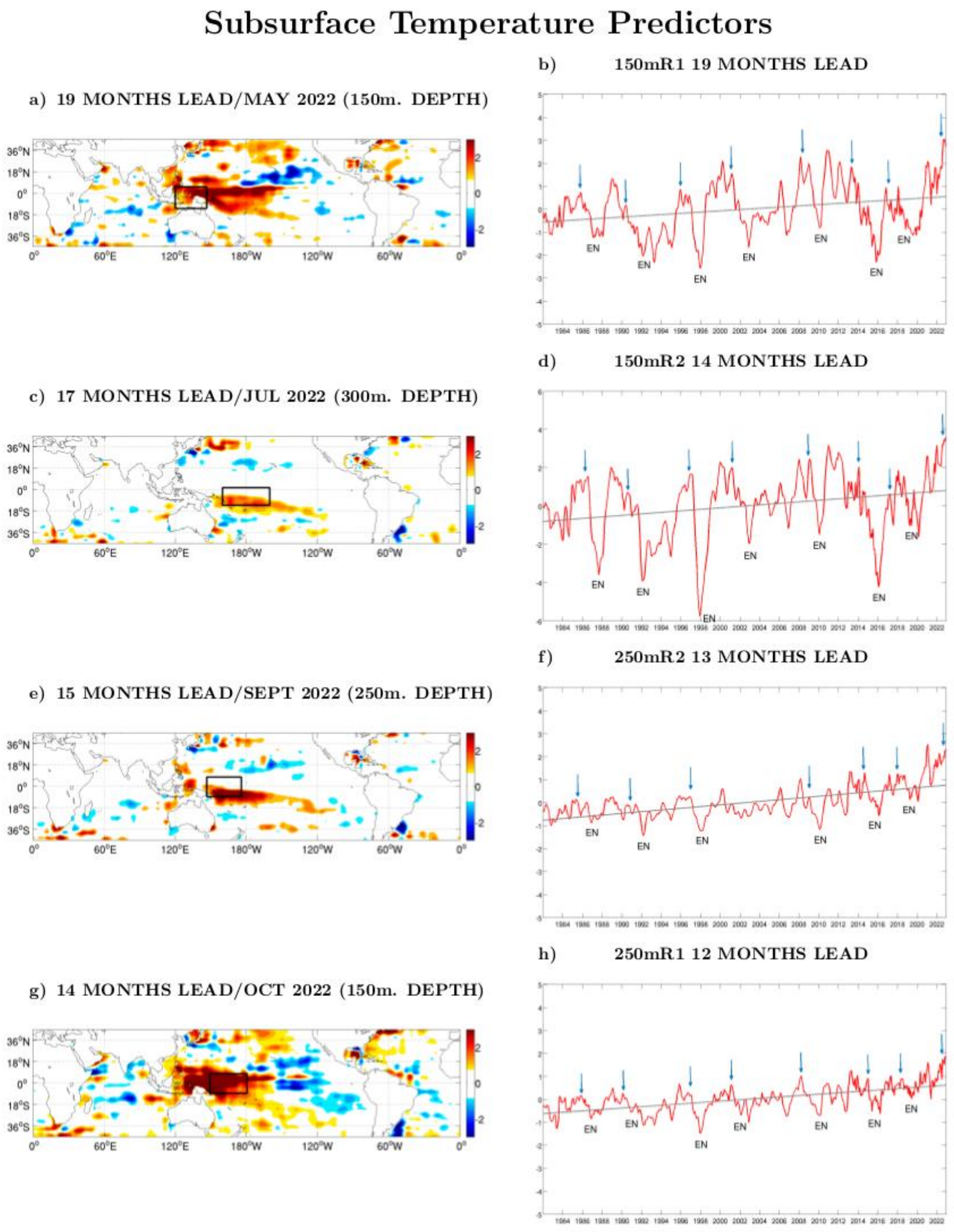
Subsurface Temperature Predictors
a) 19 MONTHS LEAD/MAY 2022 (150m. DEPTH)
b) 150mR1 19 MONTHS LEAD
c) 17 MONTHS LEAD/JUL 2022 (300m. DEPTH)
d) 150mR2 14 MONTHS LEAD
e) 15 MONTHS LEAD/SEPT 2022 (250m. DEPTH)
f) 250mR2 13 MONTHS LEAD
g) 14 MONTHS LEAD/OCT 2022 (150m. DEPTH)
h) 250mR1 12 MONTHS LEAD
EN

Fig. 3: Subsurface oceanic conditions in 2022 conducive to El Niño, and subsurface temperature time series of the predictors used in the EDCM model at different lead times. a) Temperature anomalies at 150 meters depth in May 2022, b) time series of subsurface temperature at 150 meters depth extracted from the box [10ºS-5ºN]x[120º-140ºE], c) temperature anomalies at 300 meters depth in July 2022, d) time series of subsurface temperature at 150 meters depth extracted from the box [7ºS-7ºN]x[150º-180ºE], e) temperature anomalies at 250 meters depth in September 2022, f) time series of subsurface temperature at 250 meters depth extracted from the box [7ºS-7ºN]x[140º-170ºE], g) temperature anomalies at 150 meters depth in October 2022., h) time series of subsurface temperature at 250 meters depth extracted from the box [7ºS-7ºN]x[120º-140ºE]. Black boxes in panels a, c, e and g indicate regions from which predictor time series for the model were extracted. Arrows in panels b, d, f and h indicate the time when a predictor is used for forecasting. "EN" labels indicate the time of peak El Niño conditions. Linear trend lines are included for the time series in panels b), d), f) and h) as solid grey lines.

b. ENSO forecasts for 2023/24

Figure 4 shows forecasts of SST anomalies in the Niño3.4 region initiated in January 2023 (Figure 4a), September-December 2022 (Figure 4b-e), and July 2022 (Figure 4f), corresponding to leads from 11 to 17 months along with updated observations (black solid line) until June 2024. The observed Niño3.4 values point to a moderate-to-strong EN that peaks in December 2023. All forecasts in Figure 4 predict an EN to mature in the winter of 2023/24 (Supplementary Table 3). Forecasts initiated at lead times between 11-14 months foresee a moderate warm event, but a larger EN of about 2°C amplitude is within the 70% confidence intervals of the predictions. The actual observed peak was 1.99°C. The forecast closest to this amplitude is the one issued 13 months in advance predicting a peak of 1.20°C (Supplementary Table 3). Longer-lead forecasts initiated 15 to 19 months in advance (Figure 4e and f and Supplementary Figure 2a) predict a weak EN for the winter of 2023/24. However, forecasts initiated 22 and 24 months in advance of an assumed peak in December 2023 (i.e. in the months of February 2022 and December 2021) do not predict an EN event, and show neutral conditions in the tropical Pacific instead (Supplementary Figure 2b and c), suggesting we reached a limit of feasible lead times. It is well-known especially for statistical ENSO models that the prediction of the amplitude of an event is harder and less accurate with the increase of the lead time (Barnston et al. 2012, Petrova et al. 2017, 2020 and references therein). Hence, predictions started so long in advance are likely to be incorrect, unless a very strong ENSO event is developing in the tropical Pacific. For example, in Figure 9e of Petrova et al. 2017 it can be seen that EDCM did not predict the weak 2014/15 EN at the very long lead times of 22-24 months, as opposed to Figure 4 in Petrova et al. 2020, where all strong EN events are successfully predicted even at the longer leads of 21 and 29 months in advance, albeit with a smaller amplitude than observed. We also highlight that EDCM makes use of different predictors at different lead times, and it could happen that a given predictor affected the forecast more/less strongly, and this could directly impact the amplitude of the predicted event. This could explain why EDCM predicted a higher amplitude event at 13 months, as opposed to 11 or 12 months lead time. We have seen a similar situation with the prediction of the 1997/98 EN for example (see Figure 9a and 9f in Petrova et al. 2017, where the amplitude of the event is better predicted at the very long lead times as opposed to the medium lead times). Additionally, a deterioration of the forecast precision is observed when predictions are initiated closer to the "spring predictability barrier" due to the general decrease of the signal-to-noise ratio, hence, the lower amplitudes predicted at 11 and 12 months lead time. However, the forecasted amplitudes at these leads are still greater than those predicted beyond 13 months in advance. Finally, here we used the version of EDCM that features a fixed seasonal cycle, which could explain the delay by a couple of months in the predicted peaks at all lead times (see Petrova et al. 2017 for more details on this issue).

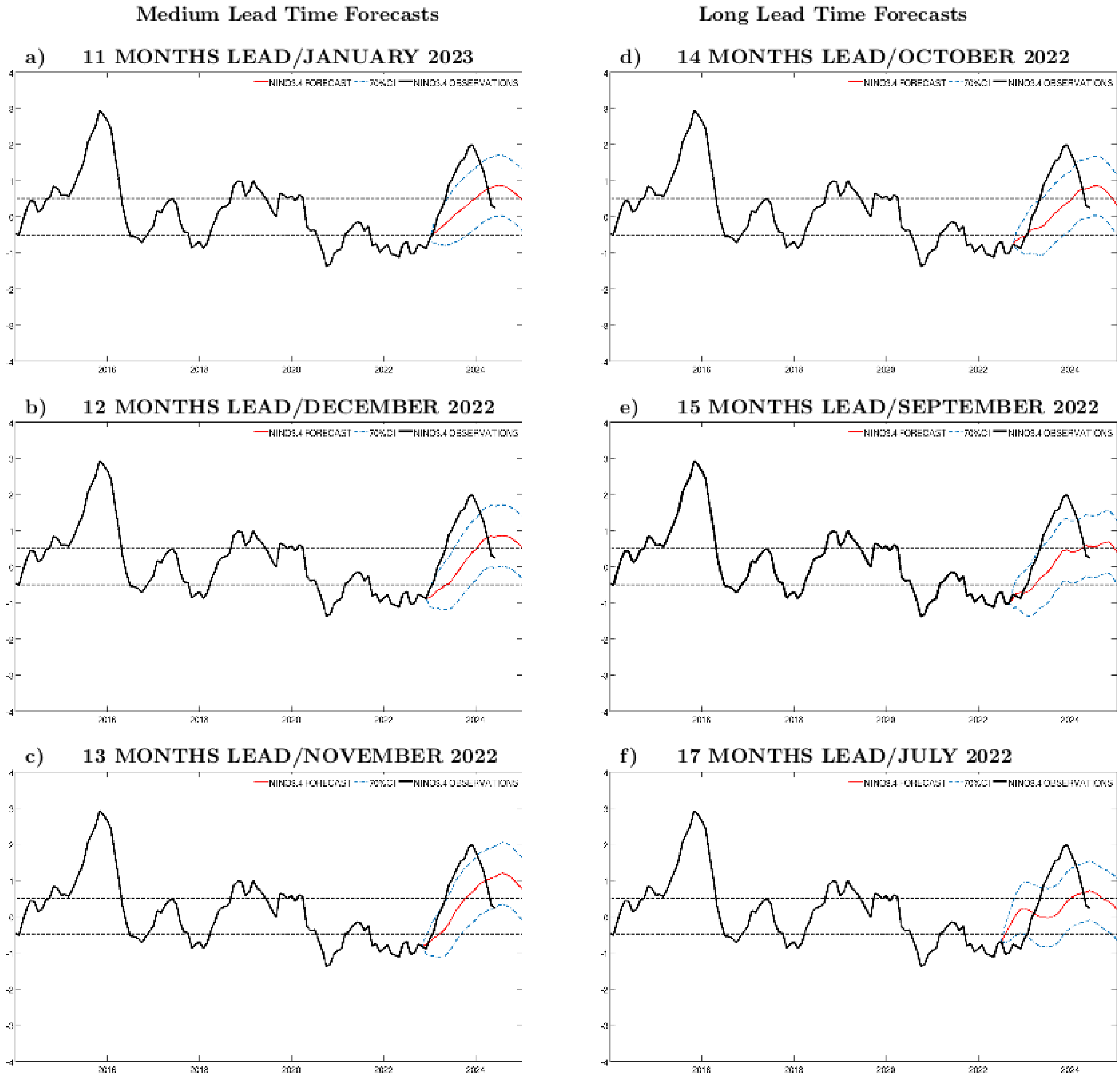

Fig. 4: Forecasts of the 2023/24 temperature anomalies [°C] in the Niño3.4 region. Forecast started in a) January 2023, b) December 2022, c) November 2022, d) October 2022, e) September 2022, f) July 2022. In all panels the thick black line is the observations (shown until

June 2024), the red line is the forecast, the blue dash-and-dotted lines are the 70% confidence intervals, and the black dotted lines are the -0.5ºC and +0.5ºC threshold for La Niña and El Niño, respectively.

4. Discussion and Conclusions

ENSO is the principal driver of climate variability, and has the potential to trigger weather- and climate-related natural and societal disasters worldwide. Climate vulnerability and the socio-economic consequences in regions where ENSO teleconnections are especially strong could be substantially reduced with the evolution of ENSO forecasts, and society has a lot to gain if ENSO predictions can be extended beyond the current operational limit of 6 months in advance. During the last several years we have designed, tested and improved EDCM, an ENSO statistical forecasting model (Petrova et al. 2017 and 2020), with the overarching goal to expand ENSO statistical predictions to at least one year ahead of the mature phase, and test the potential for even longer lead times. We were successful in hindcasting the major EN events (the 1972/73, 1982/83, 1986/87, 1997/98, 2009/10 and 2015/16 ENs) 1.5 years in advance, in some cases even 2.5 years ahead (Petrova et al. 2020). Here we showcase our forecast for the winter of 2023/24, indicating that already in October of 2022 (14 months ahead of a presumed ENSO peak in December 2023) it was possible to foresee a moderate to strong EN development in the tropical Pacific. Moreover, the model predicts the return of EN even for forecasts initiated 17 and 19 months ahead (i.e. in July and May of 2022, respectively), albeit the predicted amplitudes are for a much weaker warm event (Figure 4f and Supplementary Figure 2a).

Climate conditions in the tropical Pacific in spring-winter of 2022 were also compatible with the early onset and evolution of a warm event (Figures 1, 2 and 3), as surface temperature, zonal wind stress and subsurface temperature anomalies are all consistent with the EN preceding composite anomalies (see also Figures 6 and 7 of Petrova et al. 2017). It is interesting to note that Figures 2c and d show a decreasing trend in the zonal wind stress time series, corresponding to overall strengthening of the easterly trade winds and the Walker Circulation in the last five years (from 2018-2023). This recently observed trend change and strengthening of the zonal atmospheric circulation in the tropical Pacific, along with an enhanced warming in the WPAC region (also seen in all the time series extracted from the subsurface ocean in the WPAC in Figure 3b, d, f and h) are generally in conflict with the CMIP5 and CMIP6 climate projections for a unified warming in the equatorial Pacific, and a weakening of the Walker cell (DiNezio et al. 2013, Kociuba et al. 2015). The strengthening of the Walker circulation in recent observations has also been linked by Heede and Fedorov 2021 and 2023 to global warming as opposed to natural climate variability proposed by earlier studies (McGregor et al. 2018, Watanabe et al. 2020).

The QB and QQ modes of ENSO variability, corresponding to some of the EDCM dynamic cyclical components (along with a near annual component), are also in their growing phases in 2023 (Figure 5), signaling the high probability for an EN to occur. In Figure 5 we have extended idealized versions of these oscillatory modes, along with a decadal cycle corresponding to decadal ENSO variability (Petrova et al. 2020). These cyclical components are time-varying in the model, and their frequency and amplitude parameters can shift with changes in the overall climatic conditions, and as a result of atmospheric noise. However, we can see that in the 2023/24 winter season the idealized versions of the 2-year (QB), 4-year and 5-year cycles (QQ) are all in their peak phases. In fact, a similar superposition of these cycles occurred in 1997/98, when one of the biggest EN on record developed, despite the fact that the decadal cycle was at its trough, as it is also in 2023.

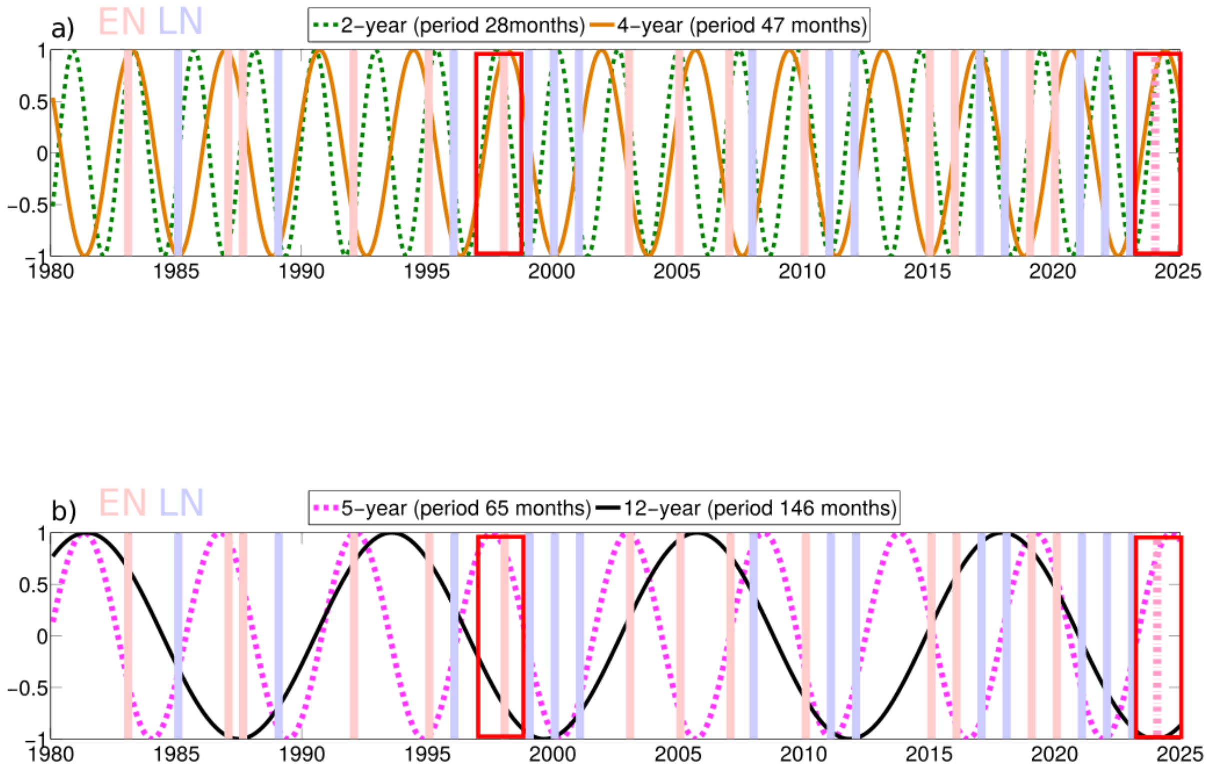

Fig. 5: Schematic of idealized oscillatory models involved in ENSO variability. Shown are cycles of periodicities corresponding to a) 2 (dashed green) and 4 (solid beige) years, b) (dashed magenta) and 12 (solid black) years. Peak months of El Niño (pink lines) and La Niña (light blue lines) from the observations are indicated. The dark pink dash-dotted line indicates the forecasted El Niño at the end of 2023. Wave amplitudes are not realistic.

For the 2023/24 winter season, our long-term predictions of 11 to 14 months in advance all suggest moderate-to-strong EN developing in the Pacific. This is a substantially longer lead time than currently used in operational forecasts. For longer 15 to 19 months lead-times, our forecasts still suggest EN development in 2023/24, albeit of weaker amplitude (Fig. 4 and Supplementary Fig. 2). Beyond these lead times, predictions initiated 22 and 24 months in advance suggested neutral conditions instead of an EN, despite the CI indicated that moderate EN conditions were possible (Supplementary Fig. 2). These results illustrate strong potential for expanding the statistical operational ENSO forecasts to 12 and 18 months in advance. Despite the fact that longer 22 and 24 months forecasts were not feasible at this instance, our success in predicting some of the previous ENSO events 2-2.5 years in advance (i.e. the 1997/98, 2002/03, 2009/10, 2015/16 ENs, See Petrova et al. 2017 and 2020), suggests that early ENSO forecasting is an avenue worth exploring further.

ENSO predictions are still constrained by the lack of complete physical understanding, parametrization of key dynamical processes, and by initialization errors due to imperfect data assimilation in the case of dynamical models, as well as by the lack of long atmospheric and oceanic historical data in the case of statistical models, in addition to the uncertainties arising from atmospheric noise (including the so-called spring barrier), and natural climate variability (Wittenberg 2009, Barnston et al. 2012, Fedorov et al. 2015). Nonetheless, this study adds to previous ones (Chen et al. 2004; Luo et al. 2008; Izumo et al. 2010; Ludescher et al. 2013, 2014; Petrova et al. 2017; Gonzalez and Goddard 2016; Ramesh et al. 2017; Luo et al. 2017; Meng et al. 2020, Petrova et al. 2020) in voicing the potential of early ENSO predictions, and call for a reconsideration and an increase of the official lead time at which operational ENSO forecasting is performed.

Clearly, the information provided by longer lead forecasts is more specific, associated with more uncertainty, and hence, suited to more specialized applications. In other words, the longer lead forecasts indicate what is more likely to happen, but are far from precise. For this reason, it is useful to explore the potential requirements of decision makers, and tailor the information provided by longer lead ENSO forecasts to those needs. For example, in health impact assessment infectious disease predictions at longer lead times based on ENSO information for diseases such as dengue and malaria could serve for saving resources and for devising optimized intervention plans to control vector infestations, and help reduce mosquito breeding sites, ultimately lowering the burden of disease and saving lives. In the area of energy production, ENSO has considerable impact on hydropower, wind power and biomass production, especially in the more affected areas in the Northwest US, South America, Central America, the Iberian Peninsula, Southeast Asia and Southeast Australia (Ng et al. 2017). The large share of hydropower electricity supply in some of these locations means that an ENSO resilient renewable energy supply will become increasingly important, and the sector would greatly benefit from long-term ENSO forecasting for a mid-term adjustment of the energy mix. Some of these systems could be adapted to apply such longer lead climate information in a probabilistic framework, so that resources could indeed be optimized, and risks properly estimated on a tailored cost-benefit basis, especially in less affluent countries and more vulnerable populations. In others the added value of knowledge so long in advance could be limited for mitigating risks related to climate variability and extremes. Therefore, such predictions should be promoted to relevant sectors in a sustainable and targeted way.

Given these considerations, it is vital to establish an operational structural framework for the issuing of such longer lead ENSO forecasts that is also based on local needs and demands. This role could be taken again by the IRI/CPC, and an additional forecasting plume could be released on a regular basis, including only models tailored for longer lead forecasts, along with a consensus ENSO outlook at a lead time of at least 1 year ahead.

In conclusion, we want to stress that ENSO forecasting has advanced to a point when useful and reliable annual timescale forecasts can be made regularly. Our results here indicated early on (already in July 2022) that an EN event was expected to mature in the winter of 2023/24. The event was predicted to be most likely moderate or strong, but in both cases the expected deviation in the global mean surface temperature as a result of the release of heat from the equatorial Pacific Ocean to the atmosphere is expected to be on the order of about 0.1°C or more (Christy and McNider 1994, Wigley 2000). Therefore, 2024 could become the next warmest year on record, and there is some likelihood that the mean increase of 1.5°C with respect to pre-industrial temperature levels set as a threshold in the Paris Climate Agreement (Christoff 2016) could be temporarily breached in the next year, should a stronger El Niño mature in the eastern tropical Pacific.

Acknowledgments.

DP and IC were supported by La Caixa Junior Leader Grant 2020 (Marie Sklodowska-Curie grant agreement No 847648). XR acknowledges support from TipESM "Exploring Tipping Points and Their Impacts Using Earth System Models ", funded by the European Union. Grant Agreement number. 101137673 DOI: 10.3030/101137673. Contribution Nr. 1. We acknowledge support from the grant CEX2023-0001290-S funded by MCIN/AEI/ 10.13039/501100011033, and support from the Generalitat de Catalunya through the CERCA Program.

Data Availability Statement.

The predictors (time series) for the ENSO model, as well as the Niño3.4 index used here, represent data that were a reanalysis of existing data, which are openly available at locations cited in the reference section. The modelling, estimation and forecasting have been carried out by the software OxMetrics/STAMP and can be downloaded from https://www.doornik.com/. A related software package is Time Series Lab and can be found at https://timeserieslab.com/.

REFERENCES

Astudillo, H. F., R. Abarca-del-Río, and F.A. Borotto, 2017: Long-term potential nonlinear predictability of El Niño–La Niña events. *Climate Dynamics*, *49*, pp.131-141.

Ballester, J., S. Bordoni, D. Petrova, and X. Rodó, 2015: On the dynamical mechanisms explaining the western Pacific subsurface temperature buildup leading to ENSO events. *Geophysical Research Letters*, *42*(8), pp.2961-2967.

Ballester, J., M.À. Rodríguez-Arias, and X. Rodó, 2011: A new extratropical tracer describing the role of the western Pacific in the onset of El Niño: Implications for ENSO understanding and forecasting. *Journal of Climate*, *24*(5), pp.1425-1437.

Ballester, J., S. Bordoni, D. Petrova, and X. Rodó, 2016: Heat advection processes leading to El Niño events as depicted by an ensemble of ocean assimilation products. *Journal of Geophysical Research: Oceans*, *121*(6), pp.3710-3729.

Barnston, A. G., M. K. Tippett, M.L. L'Heureux, S. Li, and D. G. DeWitt, 2012: Skill of real-time seasonal ENSO model predictions during 2002–11: Is our capability increasing?. *Bulletin of the American Meteorological Society*, *93*(5), pp.631-651.

Buizer, J., K. Jacobs, and D. Cash, 2016: Making short-term climate forecasts useful: Linking science and action. *Proceedings of the National Academy of Sciences*, *113*(17), pp.4597-4602.

Cane, M. A., S. E. Zebiak, and S. C. Dolan, 1986: Experimental forecasts of EL Nino. *Nature, 321*(6073), pp.827-832.

Chen, D., M. A. Cane, A. Kaplan, S. E. Zebiak, and D. Huang, 2004: Predictability of El Niño over the past 148 years. *Nature*, *428*(6984), pp.733-736.

Chen, D. and Cane, M. A., 2008: El Niño prediction and predictability. *Journal of Computational Physics*, *227*(7), pp.3625-3640.

Christy, J.R., and McNider, R.T., 1994: Satellite greenhouse signal, *Nature*, 367, pp. 325.

Clarke, A.J. and Van Gorder, S., 2003: Improving El Niño prediction using a space-time integration of Indo-Pacific winds and equatorial Pacific upper ocean heat content. *Geophysical research letters*, *30*(7).

Christoff, P., 2016: The promissory note: COP 21 and the Paris Climate Agreement. *Environmental Politics*, *25*(5), pp.765-787.

Cvijanovic, I., Santer, B.D., Bonfils, C. et al.,2017. Future loss of Arctic sea-ice cover could drive a substantial decrease in California's rainfall. *Nature Communications*, *8,* pp.1947.

DiNezio, P.N., Vecchi, G.A. and Clement, A.C., 2013. Detectability of changes in the Walker circulation in response to global warming. *Journal of Climate*, *26*(12), pp.4038-4048.

DiNezio, P. N., C. Deser, Y. Okumura, and A. Karspeck,, 2017: Predictability of 2-year La Niña events in a coupled general circulation model. *Climate dynamics*, *49*, pp.4237-4261.

Doornik, J. A. 2013: Object-Oriented Matrix Programming using Ox 7.0. Timberlake Consultants Ltd, London. http://www.doornik.com./

Durbin, J. and Koopman, S.J., 2012: *Time series analysis by state space methods* (Vol. 38). OUP Oxford.

Eisenman, I, Yu, L., Tziperman, E., 2005: Westerly wind bursts: ENSO's tail rather than the dog? *Journal of Climate*, 18, pp. 5224-5238.

Fedorov, A. V., S. Hu, M. Lengaigne, and E. Guilyardi, 2015: The impact of westerly wind bursts and ocean initial state on the development, and diversity of El Niño events. *Climate Dynamics*, *44*, pp.1381-1401.

Good, S. A., M. J. Martin, and N. A. Rayner, 2013: EN4: Quality controlled ocean temperature and salinity profiles and monthly objective analyses with uncertainty estimates. *Journal of Geophysical Research: Oceans*, *118*(12), pp.6704-6716.

Gonzalez, P. L. and Goddard, L., 2016: Long-lead ENSO predictability from CMIP5 decadal hindcasts. *Climate Dynamics*, *46*, pp.3127-3147.

Goswami, B. N. and Shukla, J., 1991: Predictability of a coupled ocean-atmosphere model. *Journal of Climate*, *4*(1), pp.3-22.

Gouretski, V. and Reseghetti, F., 2010: On depth and temperature biases in bathythermograph data: Development of a new correction scheme based on analysis of a global ocean database. *Deep Sea Research Part I: Oceanographic Research Papers*, *57*(6), pp.812-833.

Gouretski, V. and Cheng, L., 2020: Correction for systematic errors in the global dataset of temperature profiles from mechanical bathythermographs. *Journal of Atmospheric and Oceanic Technology*, *37*(5), pp.841-855.

Harvey, A. and Koopman, S. J., 2000: Signal extraction and the formulation of unobserved components models. *The Econometrics Journal*, *3*(1), pp.84-107.

Heede, U. K. and Fedorov, A. V., 2021: Eastern equatorial Pacific warming delayed by aerosols and thermostat response to CO2 increase. *Nature Climate Change*, *11*(8), pp.696-703.

Heede, U. K. and Fedorov, A. V., 2023: Colder eastern equatorial Pacific and stronger Walker circulation in the early 21st century: separating the forced response to global warming from natural variability. *Geophysical Research Letters*, *50*(3), p.e2022GL101020.

Izumo, T., J. Vialard, M. Lengaigne, C. de Boyer Montegut, S. K. Behera, J. J. Luo, S. Cravatte, S. Masson, and T. Yamagata, 2010: Influence of the state of the Indian Ocean Dipole on the following year's El Niño. *Nature Geoscience*, *3*(3), pp.168-172.

Jin, F. F., 1997: An equatorial ocean recharge paradigm for ENSO. Part I: Conceptual model. *Journal of the atmospheric sciences*, *54*(7), pp.811-829.

Kalman, R. E., 1960: A new approach to linear filtering and prediction problems. *J. Basic Eng*. March 1960; 82(1): 35–45

Kalnay, E., M. Kanamitsu, R. Kistler, W. Collins, D. Deaven, L. Gandin, M. Iredell, Saha, S., G. White, J. Woollen, and Y. Zhu, 1996: The NCEP/NCAR 40-year reanalysis project. *Bulletin of the American meteorological Society*, *77*(3), pp.437-472.

Kociuba, G. and Power, S. B., 2015: Inability of CMIP5 models to simulate recent strengthening of the Walker circulation: Implications for projections. *Journal of Climate*, *28*(1), pp.20-35.

Koopman, S. J., N. Shephard, and J. A. Doornik, 2008: Statistical algorithms for models in state space form: Ssfpack 3.0. Timberlake Consultants Press, London.

Koopman, S. J., A. C. Harvey, J. A. Doornik, and N. Shephard, 2010: Stamp 8.3: Structural time series analyser, modeller and predictor. *London: Timberlake Consultants*, *397*.

Kumar, A., Z. Z. Hu, B. Jha, and P. Peng, 2017: Estimating ENSO predictability based on multi-model hindcasts. *Climate Dynamics*, *48*, pp.39-51.

Latif, M., D. Anderson, T. Barnett, M. Cane, R. Kleeman, A. Leetmaa, J. O'Brien, A. Rosati, and E. Schneider, 1998: A review of the predictability and prediction of ENSO. *Journal of Geophysical Research: Oceans*, *103*(C7), pp.14375-14393.

L'Heureux, M. L., A. F. Levine, M. Newman, C. Ganter, J. J. Luo, M. K. Tippett, and T. N. Stockdale, 2020: ENSO prediction. *El Niño Southern Oscillation in a changing climate*, pp.227-246.

Lowe, R., A. M. Stewart-Ibarra, D. Petrova, M. García-Díez, M. J. Borbor-Cordova, R. Mejía, M. Regato, and X. Rodó, 2017: Climate services for health: predicting the evolution of the 2016 dengue season in Machala, Ecuador. *The lancet Planetary health*, *1*(4), pp.e142-e151.

Ludescher, J., A. Gozolchiani, M. I. Bogachev, A. Bunde, S. Havlin, and H. J. Schellnhuber, 2013: Improved El Niño forecasting by cooperativity detection. *Proceedings of the National Academy of Sciences*, *110*(29), pp.11742-11745.

Ludescher, J., A. Gozolchiani, M. I. Bogachev, A. Bunde, S. Havlin, and H. J. Schellnhuber, 2014: Very early warning of next El Niño. *Proceedings of the National Academy of Sciences*, *111*(6), pp.2064-2066.

Luo, J. J., S. Masson, S. K. Behera, and T. Yamagata, 2008: Extended ENSO predictions using a fully coupled ocean–atmosphere model. *Journal of Climate*, *21*(1), pp.84-93.

Luo, J. J., G. Liu, H. Hendon, O. Alves, and T. Yamagata, 2017: Inter-basin sources for two-year predictability of the multi-year La Niña event in 2010–2012. *Scientific reports*, *7*(1), p.2276.

McGregor, S., M. F. Stuecker, J. B. Kajtar, M. H. England, and M. Collins, 2018: Model tropical Atlantic biases underpin diminished Pacific decadal variability. *Nature Climate Change*, *8*(6), pp.493-498.

McPhaden, M. J. and Yu, X., 1999: Equatorial waves and the 1997–98 El Niño. *Geophysical Research Letters*, *26*(19), pp.2961-2964.

McPhaden, M. J., 2003: Tropical Pacific Ocean heat content variations and ENSO persistence barriers. *Geophysical research letters*, *30*(9).

McPhaden, M. J., 2004: Evolution of the 2002/03 El Niño. *Bulletin of the American Meteorological Society*, *85*(5), pp.677-696.

McPhaden, M. J., X. Zhang, H. H. Hendon, and M. C. Wheeler, 2006: Large scale dynamics and MJO forcing of ENSO variability. *Geophysical research letters, 33*(16).

Meng, J., J., Fan, J. Ludescher, A. Agarwal, X. Chen, A. Bunde, J. Kurths, and H. J. Schellnhuber, 2020: Complexity-based approach for El Niño magnitude forecasting before the spring predictability barrier. *Proceedings of the National Academy of Sciences*, *117*(1), pp.177-183.

Ng, J. Y., S. W. Turner, and S. Galelli, 2017: Influence of El Niño Southern Oscillation on global hydropower production. *Environmental Research Letters*, *12*(3), p.034010.

Petrova, D., S. J. Koopman, J. Ballester, and X. Rodó, 2017: Improving the long-lead predictability of El Niño using a novel forecasting scheme based on a dynamic components model. *Climate Dynamics*, *48*, pp.1249-1276.

Petrova, D., J. Ballester, S. J. Koopman, and X. Rodó, 2020: Multiyear statistical prediction of ENSO enhanced by the tropical Pacific observing system. *Journal of Climate*, *33*(1), pp.163-174.

Petrova, D., X. Rodó, R. Sippy, J. Ballester, R. Mejía, E. Beltrán-Ayala, M. J. Borbor-Cordova, G. M. Vallejo, A. J. Olmedo, A. M. Stewart-Ibarra, and R. Lowe, 2021: The 2018–2019 weak El Niño: Predicting the risk of a dengue outbreak in Machala, Ecuador. *International Journal of Climatology*, *41*(7), pp.3813-3823.

Petrova, D., J. Ballester, and X. Rodó, 2024: RossBell Dipole and PSA mode dynamics: combination forcing by ENSO and the annual cycle. Under revision in *Journal of Climate.*

Philander, S. G. H., 1983: El Niño Southern Oscillation Phenomena. *Nature*, *302*(5906), pp.295-301.

Ramesh, N., M. A. Cane, R. Seager, and D. E. Lee, 2017: Predictability and prediction of persistent cool states of the Tropical Pacific Ocean. *Climate Dynamics*, *49*, pp.2291-2307.

Ramesh, N. and Murtugudde, R., 2013: All flavours of El Niño have similar early subsurface origins. *Nature Climate Change*, *3*(1), pp.42-46.

Reynolds, R. W., N. A. Rayner, T. M. Smith, D. C. Stokes, and W. Wang, 2002: An improved in situ and satellite SST analysis for climate. *Journal of climate*, *15*(13), pp.1609-1625.

Rodó, X., M. A. Rodriguez-Arias, and J. Ballester, 2006: The role of ENSO in fostering teleconnection patterns between the tropical north Atlantic and the western Mediterranean basin. *CLIVAR Exchanges*, *11*, pp.26-27.

Ropelewski, C. F. and Halpert, M. S., 1987: Global and regional scale precipitation patterns associated with the El Niño/Southern Oscillation. *Monthly weather review*, *115*(8), pp.1606-1626.

Sarachik, E. S. and Cane, M. A., 2010: *The El Nino-southern oscillation phenomenon*. Cambridge University Press.

Torrence, C. and Webster, P. J., 1998: The annual cycle of persistence in the El Nño/Southern Oscillation. *Quarterly Journal of the Royal Meteorological Society*, *124*(550), pp.1985-2004.

Watanabe, M., J. L. Dufresne, Y. Kosaka, T. Mauritsen, and H. Tatebe, 2021: Enhanced warming constrained by past trends in equatorial Pacific sea surface temperature gradient. *Nature Climate Change*, *11*(1), pp.33-37.

Wigley, T.M.L., 2000: ENSO, volcanoes, and record-breaking temperatures, *Geophysical Research Letters*, 27, pp. 4101-4104.

Wittenberg, A. T., A. Rosati, T. L. Delworth, G. A. Vecchi, and F. Zeng, 2014: ENSO modulation: is it decadally predictable?. *Journal of Climate*, *27*(7), pp.2667-2681.

Wyrtki, K., 1975: El Niño - the dynamic response of the equatorial Pacific Ocean to atmospheric forcing. *Journal of Physical Oceanography*, *5*(4), pp.572-584.

Wyrtki, K., 1985: Water displacements in the Pacific and the genesis of El Niño cycles. *Journal of Geophysical Research: Oceans, 90*(C4), pp.7129-7132.